Article

DNA generated electric current biosensor

Lanshuang Hu, Linyan Guo, Shengqiang Hu, Congcong Shen, Minghui Yang, and Avraham Rasooly

Anal. Chem., **Just Accepted Manuscript** • DOI: 10.1021/acs.analchem.6b04756 • Publication Date (Web): 18 Jan 2017

DNA generated electric current biosensor

Lanshuang Hu[†a], Shengqiang Hu[†a], Linyan Guo[†], Congcong Shen[†], Minghui Yang[†*], Avraham Rasooly[§*]

[†]College of Chemistry and Chemical Engineering, Central South University, Changsha, China, 410083

[§]National Cancer Institute, National Institutes of Health, Rockville, MD 20850, USA

a These author contributed equally to the work

Email: yangminghui@csu.edu.cn (M. Yang)

rasoolya@mail.nih.gov (A. Rasooly)

Abstract

In addition to its primary function as a genetic material, deoxyribonucleic acid (DNA) is also a potential biologic energy source for molecular electronics. For the first time, we demonstrate that DNA can generate redox electric current. As an example of this new functionality, DNA generated redox current was used for electrochemical detection of human epidermal growth factor receptor 2 (HER2), a clinically important breast cancer biomarker. To induce redox current, the phosphate of the single stranded DNA aptamer backbone was reacted with molybdate to form redox molybdophosphate precipitate and generate an electrochemical current of ~16.8 μA/μM · cm^2. This detection of HER2 was performed using a sandwich detection assay. A HER2 specific peptide was immobilized onto a gold electrode surface for capturing HER2 in buffer and serum. The HER2 specific aptamer was used as both ligand to bind the captured HER2 and to generate a redox current signal. When tested for HER2 detection, the electrochemical current generated by the aptasensor was proportional to HER2 concentration in the range of 0.01 to 5 ng/mL, with a current generated in the range of ~6.37 to 31.8 μA/cm^2 in both buffer and serum. This detection level is within the clinically relevant range of HER2 concentrations. This method of electrochemical signal amplification greatly simplifies the signal transduction of aptasensors, broadening their use for HER2 analysis. This novel approach of using the same aptamer as biosensor ligand and as transducer can be universally extended to other aptasensors for a wide array of biodetection applications. Moreover, electric currents generated by DNA or other nucleic acids can be used in molecular electronics or implanted devices for both power generation and measurement of output.

Graphic presentation.

DNA generated redox electric current: *The DNA current generation is based on the reaction of phosphate groups (P) with molybdate (M) that can form redox molybdophosphate precipitate (MP) and generate electrochemical current (EC). Since DNA comprises a backbone made from deoxyribose (S) and phosphate groups (P), the reaction of DNA with molybdate generated electrochemical current (EC).*

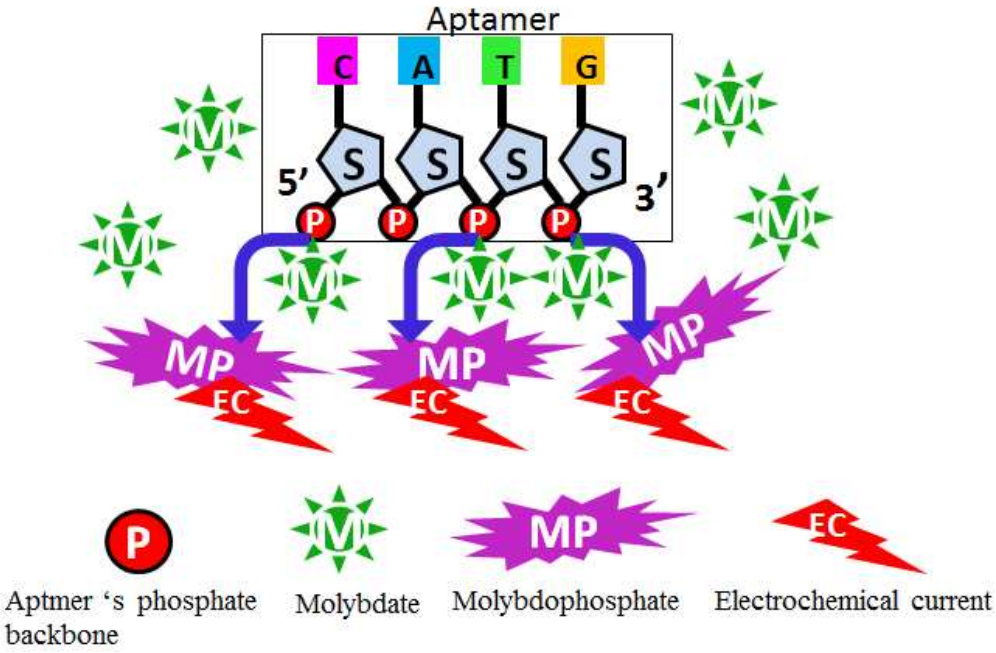

INTRODUCTION

The primary function of DNA is to store the genetic information of the cell. Due to its unique physical and biological properties, DNA also has the potential for applications in molecular electronics, including DNA-based electrical circuits. Molecular scale electronics use single molecules as electronic components, enabling miniaturization to molecular dimensions for uses as varied as signal gating via molecular transistors, and molecular recognition for both switching as well as sensing capabilities. Molecular scale electronics have the potential to overcome the limitations of conventional silicon-based integrated circuits, enabling Moore's law to be extended beyond the limits of conventional electronics.[1] DNA has been utilized in molecular electronics to conduct charge[2-6] and for logic gating.[7,8] DNA is also used for label free detection. In addition, we hypothesize that DNA can be used as a biological electric current source using the chemical energy stored in its bonds or the electrical charge of the molecules on the DNA phosphate backbone. It has been shown that phosphate can react with molybdate to induce redox electric current [9-11], the equation regarding the reaction of phosphate with molybdate (equation 1) and redox reaction of molybdophosphate (equation 2 and 3) measured at the electrochemical electrode surface are displayed below:

$$12MoO_4^{2-} + 24\ H^+ + PO_4^{3-} \rightarrow PMo_{12}O_{40}^{3-} + 12\ H_2O \qquad (1)$$

$$PMo_{12}O_{40}^{3-} + 2e + 2H^+ \rightarrow H_2PMo_2^{V}\ Mo_{10}^{VI}\ O_{40}^{3-} \qquad (2)$$

$$H_2PMo_2^{V}Mo_{10}^{VI}O_{40}^{3-} + 2e + 2H^{+} \rightarrow H_4PMo_4^{V}Mo_8^{VI}O_{40}^{3-} \quad (3)$$

We hypothesize that the phosphate in DNA (or in any nucleic acid) backbone can also generate redox electric current. To test this hypothesis we used an aptamer for the breast cancer marker human epidermal growth factor receptor 2 (HER2) to generate a redox electric current for an electrochemical biosensor designed for detection of HER2.

Biosensors have two main elements, the ligand which serves as recognition element binding to the target, and a transducer which generates a signal resulting from the ligand binding. Here we combine these two elements into a single aptamer which serves both as ligand to bind HER2 and transducer to generate electrochemical redox electric current signal.

Aptamers are a class of small nucleic acid (RNA or single-stranded DNA) or peptide with high specificity and affinity for their targets, which are used as ligands as an alternative to traditional antibodies.[12,13] Aptamers are isolated through SELEX (systematic evolution of ligands by exponential enrichment) and can be easily prepared *via* a solid-phase oligonucleotide synthesis with good reproducibility.[14-16] The binding targets of aptamers include biomarker proteins, small molecules and even whole-live cells, making the use of such synthetic ligands attractive for biosensing and therapeutics.[17-24]. However, for biosensing applications, signal tags need to be modified on the aptamer for signal amplification. Thus, it is advantageous to develop aptasensors utilizing the aptamer both as ligand and as signal tag based on aptamer structure and

chemical properties. Among the many applications of such an approach, detection of a breast cancer marker is a critical application.

Breast cancer is a major health concern, affecting about 12% of women in the U.S during their lifetime. In 2016 more than 246,600 new cases of invasive breast cancer are expected to be diagnosed in women in the U.S. The effectiveness of cancer treatment relies on cancer detection and diagnosis, one of the clinical markers used for breast cancer diagnosis is HER2. The *HER2* gene controls production of the HER2 protein and is overexpressed in around 20–30% of breast cancer tumors and is associated with a more aggressive disease, higher recurrence rates, and increased mortality.[25] Chemotherapy and targeted therapy may be effective in treatment of these cancers. HER2-targeted therapies including lapatinib (Tykerb), trastuzumab (Herceptin), pertuzumab (Perjeta), and ado-trastuzumab emtansine (T-DM1; Kadcyla) are effective only against HER2-positive tumor cells but are ineffective for HER2 negative invasive cancers. In addition, these drugs may cause serious side effects including liver inflammation, heart problems, diarrhea, and skin problems. So to avoid ineffective treatment, HER2 status is an important prognostic and predictive breast cancer marker.[26-29] Currently there are two FDA-approved HER2 analysis methods, immunohistochemistry (IHC) to detect HER2 protein on the cancer cell surface and fluorescence in situ hybridization (FISH) DNA probes to determine the number of copies of the *HER2* gene in the tumor cells. However, IHC and FISH require invasive biopsy tissue sample which have some risk and may not be practical for cancer monitoring. Moreover, these laboratory tests require medical infrastructure,

pathology and cytology expertise not available in many parts of the world, especially in low resource settings. In addition to cellular HER2 analysis, it was shown that HER2 extracellular domain shaded from cell surface and detected in serum and the association of HER2 serum level with tumor burden was suggested.[30-33] The serum concentration was elevated in 20%–50% of patients with primary breast cancer and 50%–62% for metastatic disease.[34,35] Normal individuals have a HER2 concentration between 2 and 15 ng⁄ml in the blood and breast cancer patients have blood HER2 levels from 15 to 75 ng⁄ml.[36]

These and other data suggest that measurement of HER2 in serum may have prognostic and predictive value of great clinical utility. The American Medical Association (AMA) has approved a serum HER-2/neu oncoprotein test (CPT code 83950) intended to quantitatively measure HER-2/neu protein in serum of women with metastatic breast cancer as a complement to conventional invasive tissue testing such as IHC or FISH. This test can determine a woman's HER-2 status, predict response to therapy and monitor therapeutic response. The non-invasive serum monitoring is intended to provide "real time HER2 level information with Reference Range(s)<12.8 ng/mL". Electrochemical biosensors are widely used for immunoassays and they can be used in a variety of settings ranging from clinical and research laboratories to home diagnostics and use in low resource or global health settings lacking developed medical infrastructure and medical expertise. For HER2 detection, biosensors were reported utilizing peptides and oligonucleotides as ligands [37-39] [40]. In this work, we describe a novel approach for DNA generated redox electric current for HER2 electrochemical

detection which can be used for biodetection and for powering and measuring output in molecular electronics and for implanted devices.

EXPERIMENTAL SECTION

Materials and reagents: The peptide (CKLRLEWNR) was obtained from GL Biochem Ltd (Shanghai, China). The aptamer with a sequence of 5′-GCA GCG GTG TGG GG-3′ was synthesized and purified by Sangon Biotech Co., Ltd. (Shanghai, China). Human epidermal growth factor receptor-2 (HER2) was acquired from Abcam Co., Ltd. (Cambridge, MA, USA). Sodium molybdate dihydrate ($Na_2MoO_4{\cdot}2H_2O$) and 6-mercapto-1-hexanol (MCH) were purchased from Sigma-Aldrich (St. Louis, MO, USA). Human serum was purchased from Zhenglong Biochem. Lab (Chengdu, China). Other reagents were of analytical grade and used without further purification. All stock solutions were prepared with deionized water.

Electrochemical Apparatus: Electrochemical measurements were performed on a CHI-650D electrochemical workstation (Shanghai CH Instruments Co., China). A conventional three-electrode system was used with a gold electrode (2 mm in diameter) as the working electrode, a saturated calomel electrode as the reference electrode and a platinum wire as the auxiliary electrode.

Preparation of the aptasensor: To prepare the aptasensor, a gold electrode was immersed into10 μg/mL of the peptide solutions at 37 ℃ overnight to link the peptide to the gold electrode. After extensive washing, 1 mM of the MCH was added onto the electrode for 0.5 h to block sites that may cause nonspecific adsorption. Subsequently, different concentrations of HER2 were added onto the electrode surface and incubated at 37 ℃ for 1 h. After washing, 100 μM of the aptamer solutions was applied to the

electrode at 37 ℃ for another 1 h, followed by washing with deionized water to remove nonspecific adsorbed DNA. Finally, 5 μL of 1 mM Na_2MoO_4 solutions were dripped onto the electrode surface for 20 min prior to electrochemical characterization.

RESULTS AND DISCUSSION

DNA generated electric current

The DNA or other nucleic acid electric current generation strategy is based on previous work demonstrating that the reaction of phosphate with molybdate can form redox molybdophosphate precipitate and generate electrochemical current.[9-11] Our model for DNA generated electric power suggest that since the DNA backbone is comprised of deoxyribose and phosphate groups, the reaction of DNA with molybdate could form redox molybdophosphate precipitate and generate electrochemical current.

To study DNA electric current generation, oligonucleotides with different nucleobases were reacted with molybdate and the electric current was measured. Solution containing 100 μM 12 polycytosine oligonucleotide (dC_{12}) was reacted with 1 mM of molybdate on the electrode surface for 20 min and then the electrode was characterized. In 0.5 M H_2SO_4, the cyclic voltammograms (CV) of the electrode displays two pairs of redox peaks at around 0.22 V and 0.32 V, respectively, which are ascribed to electron-transfer between different states of Mo in the formed molybdophosphate ($PMo_{12}O_{40}$) precipitates (Fig. 1A, curve a). A control experiment with only 100 μM of dC_{12} resulted in no redox peaks (Fig. 1A, curve b). These data

indicated the reaction of dC_{12}, specifically, the reaction of phosphate groups contained in the dC_{12} with molybdate leads to the formation of molybdophosphate precipitate on the electrode surface as described in equation 1-3.[9-11] We also tested DNA oligonucleotide composed of other nucleobases. Square wave voltammogram (SWV) curves in Fig. 1B shows that for the same concentrations of oligonucleotide (100 μM), compared to dC_{12} DNA oligonucleotide, DNA oligonucleotide composed of 12 T or 12 A nucleobases exhibited much lower electrochemical current as well as DNA oligonucleotide composed of 6 G and 6 C nucleobases. Since the DNA strands comprise both nucleobases and a deoxyribose-phosphate backbone, we think different nucleobase sequences resulted in the alteration of the backbone. These different backbones may leads to variation of phosphate group amounts and therefore the resulting electrochemical current. Finally, oligonucleotide with sequence GCAGCGGTGTGGGG used as aptamer for human epidermal growth factor receptor 2 (HER2) resulted in a similar redox profile (Fig. 1C), demonstrating the possibility of using aptamer both as recognition and signal probe. In addition, SWV curves demonstrated the peak current was increased with the increase of aptamer concentrations (Fig. 1D). The insert in Fig. 1D shows high correlation between the concentrations of aptamer and generated current. The generated current at 0.2 V was linearly related to the logarithm of aptamer concentration in the range from 0.001 to 10 μM (R=0.998) with current intensity around 16.8 $\mu A/\mu M \cdot cm^2$.

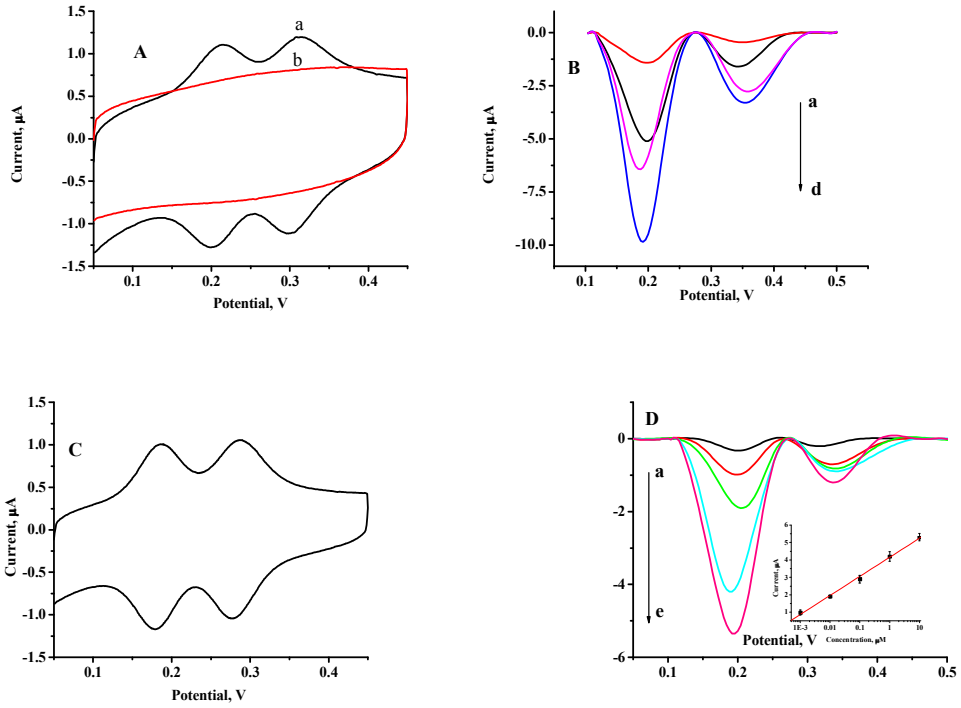

Fig. 1 DNA generated redox electric current: *Oligonucleotides were immobilized onto gold electrode and the current was measured. (A) CVs of* dC_{12} *modified electrode after reaction with molybdate (a) and without reaction with molybdate (b); (B) SWV responses of various DNA oligonucleotides modified electrode after reaction with molybdate, from a to d,* dA_{12}, dG_6+C_6, dT_{12} *and* dC_{12}*; (C) CV of HER2 aptamer modified electrode after reaction with molybdate; (D) SWV responses of different concentrations of HER2 aptamer modified electrode after reaction with molybdate, from a to e, 0, 0.001, 0.01, 1 and 10 μM. Supporting electrolyte, 0.5 M* H_2SO_4.

Electrochemical aptasensor for HER2 detection. To demonstrate the utility of DNA generated current we developed an aptasensor for the detection of HER2. Our aptasensor for HER2 is based on a "sandwich" configuration with HER2 peptide as a

primary capturing ligand and HER2 aptamer as a secondary capturing ligand as well as signal generator. To prepare the aptasensor (Fig 2), a gold electrode was immersed in the peptide solutions to link the peptide to the gold electrode. After extensive washing, MCH was added to block sites that may cause nonspecific adsorption. Subsequently, the electrode was incubated sequentially with different concentrations of HER2, followed by aptamer solution and then the Na_2MoO_4 solution to generate signal.

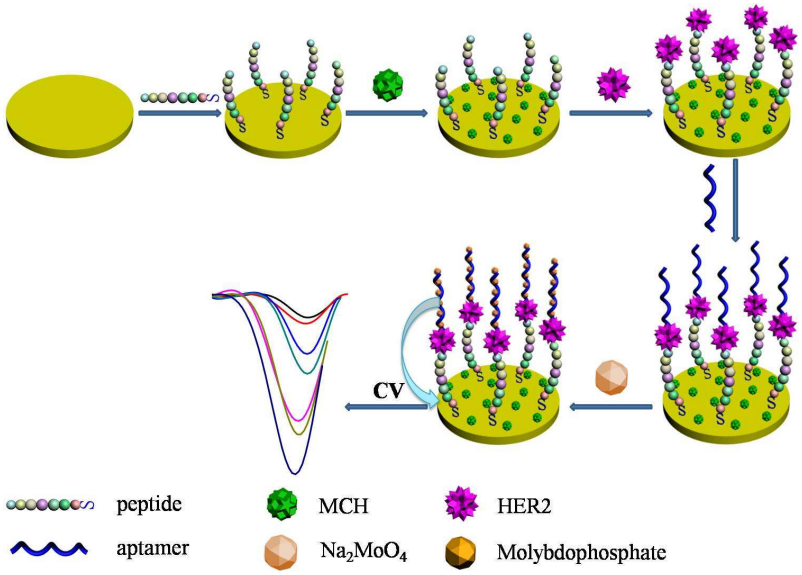

Figure 2. Aptasensor assembly: *the primary capturing peptide was attached to the bare gold electrode. MCH was added to block nonspecific adsorption followed by HER2 binding and aptamer binding. Aptamer was utilized as secondary ligand for signal generation when reacted with molybdate to form redox molybdophosphate precipitate and to generate electrochemical current.*

The sensor assembly process was characterized in $[Fe(CN)_6]^{3-/4}$ solution (Fig 3A). After the first step of assemble of HER2 specific peptide onto the gold electrode, the

current peak of the electrode was decreased compared to a bare electrode due to the formed peptide layer partially blocking electron transfer at the electrode surface. With the following capture of HER2 molecules, and especially the capture of HER2 aptamer, the peak current was decreased again, which can be ascribed to the negatively charged aptamer strands that repelled $[Fe(CN)_6]^{3-/4}$ ions from the electrode These results prove the successful preparation of the aptasensor.

In addition, after each assembly step, the reaction of the aptasensor with molybdate was studied. Fig.3B shows SWV curves of the modified sensor in 0.5 M H_2SO_4 after reaction with molybdate. From the curves, it can be seen that in comparison to bare gold electrode in H_2SO_4 (curve a), molybdate itself can generate a small peak current on the bare electrode surface (curve d). The current intensity was decreased with the modification of peptide on the electrode, and further decreased after the capture of 5 ng/mL of HER2 on the electrode (curve b and c). The current intensity was decreased because the peptide and HER2 layer prevented contact of molybdate with the electrode. However, after the capture of HER2 aptamer, there is a substantial enhancement of the current intensity (curve e). In particular, the current peak at 0.2 V was about 7 times higher than that before the capture of aptamer. The enhanced current can be ascribed to aptamer induced redox current after reaction of aptamer with molybdate, demonstrating the possible applicability of the aptasensor to HER2 detection.

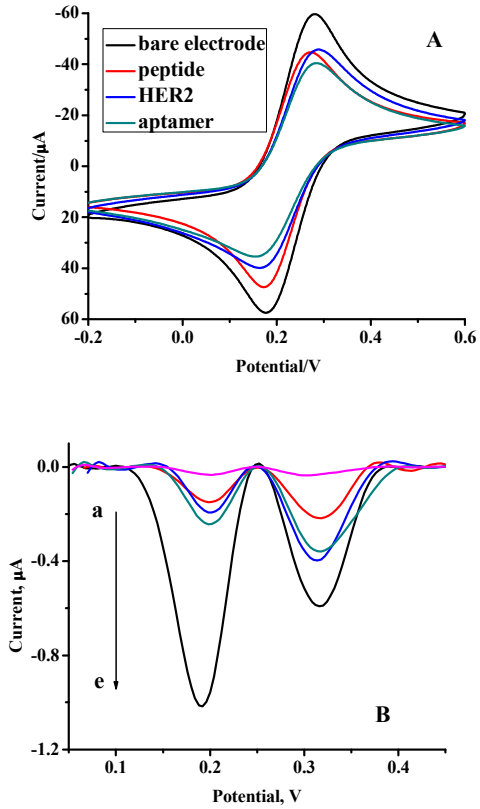

Figure 3, Tracking aptasensor assembly and detection process A. Aptasensor assembly: *SWV measurements of the assembly steps of the aptasensor in* $[Fe(CN)_6]^{3-/4}$ *solution, measured after each assemble step.* ***B. Aptasensor measurements with molybdate:*** *SWV responses of electrodes in 0.5 M* H_2SO_4*, (a) bare electrode; (b) peptide and 5 ng/mL of HER2 modified electrode after reaction with molybdate; (c) peptide modified electrode after reaction with molybdate; (d) bare electrode after reaction with molybdate; (e) peptide, 5 ng/mL of HER2 and aptamer modified electrode after reaction with molybdate.*

Aptasensor detection of HER2. Different concentrations of HER2 were then analyzed by the aptasensor to test the linear range of the aptasensor to HER2. As can be seen from Fig. 4A, the SWV peak current of the sensors at 0.2 V was increased with the increase of HER2 concentrations. The increased current resulted from

increased concentration of HER2, more aptamer molecules are captured onto electrode through specific binding between HER2 and the aptamer. There is a linear relationship between the generated peak current and the logarithm of HER2 concentration in the range from 0.01 to 5 ng/mL with current intensity increased from 6.37 to 31.8 μA/cm^2 (inset of Fig. 4A). The detection limit was 5 pg/mL based on S/N = 3. The concentrations of HER2 in breast cancer patients are in the range of 15–75 ng/mL compared to 2–15 ng/mL for normal individuals. The AMA clinical Reference Range(s)<12.8 ng/mL in serum of women with metastatic breast cancer suggest that the apatsensor has enough sensitivity for the detection of HER2 in diluted samples.[40]

Selectivity and Reproducibility of HER2 electrochemical aptasensor. Other analytical parameters of the aptasensor, such as selectivity and reproducibility were studied. Good selectivity is of great importance for the precise detection of analyte target in real samples. To test the selectivity of the aptasensor, several other protein biomarkers were selected as potential interferents, such as Human IgG, carcinoembryonic antigen (CEA), mucin 1 (MUC1) and p53. The responses of the aptasensor to 5 ng/mL of the above interfering protein were negligible compared to that of 5 ng/mL of HER2, indicating good selectivity of the aptasensor (Fig. 4B). The good selectivity of the sensor can be ascribed to the intrinsic selectivity of the peptide sequence and aptamer to HER2 molecules. In addition, to study the reproducibility of the aptasensor, 100 pg/mL of HER2 were tested independently for four times. The relative standard deviation (RSD) of the result was 3.9%, proving the testing results were quite reproducible.

Detection of the HER2 in serum using the aptasensor. To demonstrate the potential application of the aptasensor for testing HER2 in human serum, we measured HER2 in serum. Into diluted human serum samples, various concentrations of HER2 were added. The samples were then tested by the aptasensor as described above. The signal in serum without HER2 is about 0.19 μA and the results of the HER2 measurements in serum are shown in Fig. 4C, which indicate that there is no significant difference between HER2 measurements in serum compared to measurements in buffer. There is a linear relationship between the peak current and logarithm of HER2 concentration in serum in the range from 0.01 to 5 ng/mL meeting the AMA clinical Reference Range(s)<12.8 ng/mL, suggesting that the aptasensor can detect HER2 in diluted serum samples.

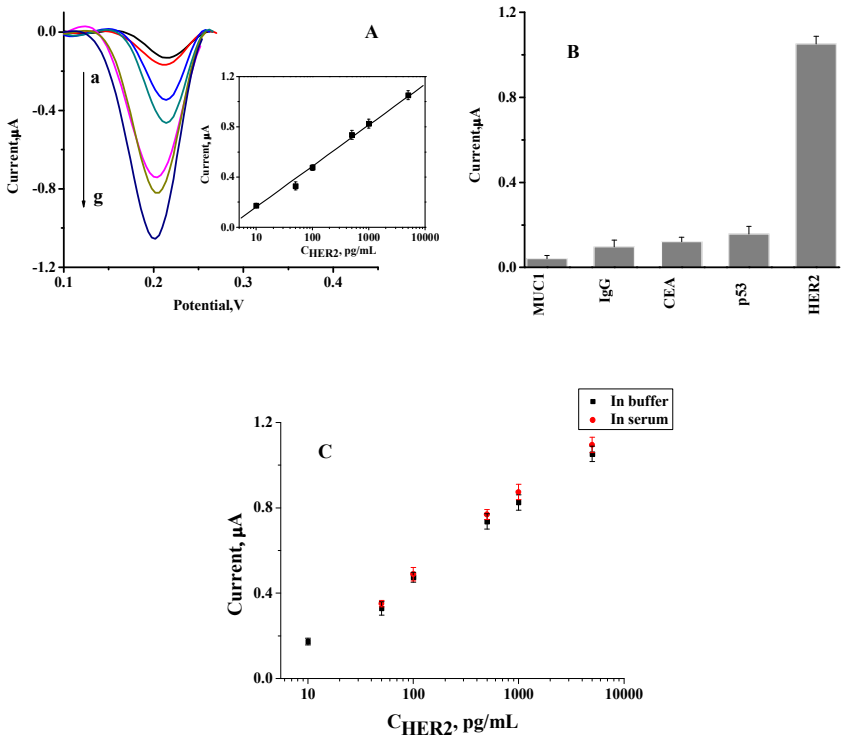

Fig. 4 HER2 electrochemical aptasensor A*. SWV responses of aptasensor to different concentrations of HER2, from a to g, 0, 0.01, 0.05, 0.1, 0.5, 1, 5 ng/mL. The inset is the calibration curve of the aptasensor to HER2.* ***B.*** *Selectivity of HER2 electrochemical aptasensor. Response of the aptasensor to 5 ng/mL of different proteins including human IgG, carcinoembryonic antigen (CEA), mucin 1 (MUC1) and p53.* ***C.*** *Measurement of HER2 in human serum. Human serum samples were diluted and spiked with different concentrations of HER2, and the serum samples were then tested by the aptasensor. Detection of HER2 in human serum (red) and in standard buffer (black).*

CONCLUSION

In an electrochemical reaction, HER2 aptamer generated electric current of 16.8 μA/μM . cm^2. Several biomedical applications use low current, for example, most pacemakers draw 10–30 μA from a battery. So theoretically DNA generated current can be used for biological pacing to treat arrhythmias. In addition the current level is in the μA range of microcurrent electrical neuromuscular stimulator (MENS) used to send weak electrical signals into the body for treatments for pain, regeneration of injured skeletal muscle and other treatments.[41] Such low power MENS can improve tissue repair in patients and promotes reverse remodelling in cardiomyocytes caused by imbalances in the extracellular matrix composition which may induce manifestation of heart failure.[42]

This current can also be used for powering molecular electronics, expanding the role of DNA in molecular electronics beyond its current applications of conducting charge and for logic gating. The combination of aptamer with a secondary DNA structure may enable use of DNA as an electronic switch for molecular electronics

controlled by the structural change induced by aptamer/target binding. A possible clinical utility for such aptamer switch is for preventing heart attacks. With monitoring of blood, high levels of cardiac biomarkers such as cardiac troponin or creatinine kinase (CK) are correlated with heart attack, so the system can be used as a molecular switch to turn on for an early alarm for heart attack, enabling corrective measure before the heart attack or even as a molecular switch for automated implanted medical devices. Thus there are many potential biomedical applications for use of DNA as an energy source and DNA controlled molecular electronics.

In addition to the ability to generate electric current, our approach may improve biosensing. While aptamers are usually used as ligands for biosensors, in our aptasensor strategy we used the same aptamer as a biosensor ligand to capture HER2 and as a transducer to induce redox current for HER2 measurement.

In recent years many biosensors has been developed including a simplified Field-effect capacitive electrolyte–insulator–semiconductor (EIS) which has been applied for a label-free electrostatic detection of charged molecules by their intrinsic molecular charge or for real-time in situ electrical monitoring of the layer-by-layer formation of polyelectrolyte (PE) multilayers [43] [44]. As a biosensor, the new DNA based sensor may greatly simplify the signal transduction of aptasensors utilizing aptamer both as recognition and signal probe for biosensors. For the detection of the breast cancer biomarker HER2, the aptasensor displays a wide linear range from 0.01 ng to 5 ng/mL in both buffer and serum, while the clinical Referencef Range(s) for

HER2 is below 12.8 ng/mL, which suggest that the apatsensor has sufficient sensitivity for the detection of HER2 in diluted samples. The aptasensor also displayed good selectivity and reproducibility for HER2 detection, suggesting potential clinical utility.

While there are many potential long term biomedical applications for DNA generated current, the new biosensor approach presented here may broaden the use of HER2 analysis and enable effective breast cancer treatment for low resource settings and for global health. Moreover, the strategy of using the same aptamer both as biosensor ligand and as a transducer could be useful in a wide array of other biosensing applications and enable simplification of biosensing.

ACKNOWLEDGMENTS

The authors thank the support of this work by the National Key Basic Research Program of China (2014CB744502), the National Natural Science Foundation of China (No. 21575165) and the Natural Science Foundation of Hunan province (No. 2015JJ1019).

References

(1) Jackson, T. N. *Nat Mater* **2005**, *4*, 581-582.
(2) Slinker, J. D. M., N. B.; Renfrew, S. E.; Barton, J. K. *Nat Chem* **2011**, *3*, 228-233.
(3) Genereux, J. C. B., J. K. *Nat Chem* **2009**, *1*, 106-107.
(4) Kawai, K. K., H.; Osakada, Y.; Majima, T. *Nat Chem* **2009**, *1*, 156-159.
(5) Xiang, L. P., J. L.; Bruot, C.; Mujica, V.; Ratner, M. A.; Tao, N. *Nat Chem* **2015**, *7*, 221-226.

(6) Wardrip, A. G. M., A.; Husken, N.; Jocson, J. M.; Bartlett, A.; Lopez, R. C.; Frey, N.; Markegard, C. B.; Kladnik, G.; Cossaro, A.; Floreano, L.; Verdini, A.; Burke, A. M.; Dickson, M. N.; Kymissis, I.; Cvetko, D.; Morgante, A.; Sharifzadeh, S.; Nguyen, H. D.; Gorodetsky, A. A. *Angew Chem Int Ed Engl* **2016**.
(7) Artes, J. M. L., Y.; Qi, J.; Anantram, M. P.; Hihath, J. *Nat Commun* **2015**, *6*, 8870.
(8) Gao, W. Z., L.; Liang, R. P.; Qiu, J. D. *Chemistry* **2015**, *21*, 15272-15279.
(9) Shen, C.; Li, X.; Rasooly, A.; Guo, L.; Zhang, K.; Yang, M. *Biosensor. Bioelectron.* **2016**, *85*, 220-225.
(10) Xie, S.; Yuan, Y.; Chai, Y.; Yuan, R. *Anal. Chem.* **2015**, *87*, 10268-10274.
(11) Qu, F.; Yang, M.; Rasooly, A. *Anal. Chem.* **2016**.
(12) Chen, T.; Shukoor, M. I.; Chen, Y.; Yuan, Q.; Zhu, Z.; Zhao, Z.; Gulbakan, B.; Tan, W. *Nanoscale* **2011**, *3*, 546-556.
(13) Meng, H.-M.; Fu, T.; Zhang, X.-B.; Tan, W. *Nat. Sci. Rev.* **2015**, *2*, 71-84.
(14) Wang, R.; Lu, D.; Bai, H.; Jin, C.; Yan, G.; Ye, M.; Qiu, L.; Chang, R.; Cui, C.; Liang, H.; Tan, W. *Chem. Sci.* **2016**, *7*, 2157-2161.
(15) Liang, C.; Guo, B.; Wu, H.; Shao, N.; Li, D.; Liu, J.; Dang, L.; Wang, C.; Li, H.; Li, S.; Lau, W. K.; Cao, Y.; Yang, Z.; Lu, C.; He, X.; Au, D. W. T.; Pan, X.; Zhang, B.-T.; Lu, C.; Zhang, H.; Yue, K.; Qian, A.; Shang, P.; Xu, J.; Xiao, L.; Bian, Z.; Tan, W.; Liang, Z.; He, F.; Zhang, L.; Lu, A.; Zhang, G. *Nat. Med.* **2015**, *21*, 288-+.
(16) Pu, Y.; Liu, Z.; Lu, Y.; Yuan, P.; Liu, J.; Yu, B.; Wang, G.; Yang, C. J.; Liu, H.; Tan, W. *Anal. Chem.* **2015**, *87*, 1919-1924.
(17) Yi, M.; Yang, S.; Peng, Z.; Liu, C.; Li, J.; Zhong, W.; Yang, R.; Tan, W. *Anal. Chem.* **2014**, *86*, 3548-3554.
(18) Yuan, Q.; Wu, Y.; Wang, J.; Lu, D.; Zhao, Z.; Liu, T.; Zhang, X.; Tan, W. *Angew. Chem. Int. Ed.* **2013**, *52*, 13965-13969.
(19) Wu, C.; Chen, T.; Han, D.; You, M.; Peng, L.; Cansiz, S.; Zhu, G.; Li, C.; Xiong, X.; Jimenez, E.; Yang, C. J.; Tan, W. *ACS Nano* **2013**, *7*, 5724-5731.
(20) Zhang, J.; Liu, B.; Liu, H.; Zhang, X.; Tan, W. *Nanomedicine* **2013**, *8*, 983-993.
(21) Wang, Z.; Yu, J.; Gui, R.; Jin, H.; Xia, Y. *Biosensor. Bioelectron.* **2016**, *79*, 136-149.
(22) Zhang, K.; Wang, K.; Zhu, X.; Xie, M. *Biosensor. Bioelectron.* **2016**, *78*, 154-159.
(23) Yang, M.; Yi, X.; Wang, J.; Zhou, F. *Analyst* **2014**, *139*, 1814.
(24) Neves, M. A. D.; Blaszykowski, C.; Thompson, M. *Anal. Chem.* **2016**, *88*, 3098-3106.
(25) Mitri, Z. C., T.; O'Regan, R. *Chemother Res Pract* **2012**, *2012*, 743193.
(26) Ross, J. S.; Fletcher, J. A. *Oncologist* **1998**, *3*, 237-252.
(27) Eppenberger-Castori, S. K., W.; Benz, C.; Caduff, R.; Varga, Z.; Bannwart, F.; Fink, D.; Dieterich, H.; Hohl, M.; Muller, H.; Paris, K.; Schoumacher, F.; Eppenberger, U. *J Clin Oncol* **2001**, *19*, 645-656.
(28) Tsongalis, G. J. R., A., Jr. *Crit Rev Clin Lab Sci* **2001**, *38*, 167-182.
(29) Ross, J. S. F., J. A. *Stem Cells* **1998**, *16*, 413-428.
(30) Tokuda, Y. W., T.; Omuro, Y.; Ando, M.; Katsumata, N.; Okumura, A.; Ohta, M.; Fujii, H.; Sasaki, Y.; Niwa, T.; Tajima, T. *Br J Cancer* **1999**, *81*, 1419-1425.
(31) Molina, R. A., J. M.; Escudero, J. M.; Filella, X.; Zanon, G.; Pahisa, J.; Farrus, B.; Munoz, M.; Velasco, M. *Tumour Biol* **2010**, *31*, 171-180.
(32) Robertson, J. F. J., W.; Syzmendera, J. J.; Selby, C.; Coleman, R.; Howell, A.; Winstanley, J.; Jonssen, P. E.; Bombardieri, E.; Sainsbury, J. R.; Gronberg, H.; Kumpulainen, E.; Blamey, R. W. *Eur J Cancer* **1999**, *35*, 47-53.
(33) Kurebayashi, J. N., R.; Tanaka, K.; Kohno, N.; Kurosumi, M.; Moriya, T.; Ogawa, Y.; Taguchi, T. *Breast Cancer* **2004**, *11*, 389-395.

(34) Fehm, T. G., G.; Jager, W. *Breast Cancer Res Treat* **2002**, *75*, 97-106.
(35) Dittadi, R. Z., M.; Perasole, A.; Gion, M. *Int J Biol Markers* **2001**, *16*, 255-261.
(36) Meenakshi, A. K., R. S.; Kumar, N. S. *J Immunoassay Immunochem* **2002**, *23*, 293-305.
(37) Wang, Z.; Wang, W.; Bu, X.; Wei, Z.; Geng, L.; Wu, Y.; Dong, C.; Li, L.; Zhang, D.; Yang, S.; Wang, F.; Lausted, C.; Hood, L.; Hu, Z. *Anal. Chem.* **2015**, *87*, 8367-8372.
(38) Loo, L.; Capobianco, J. A.; Wu, W.; Gao, X.; Shih, W. Y.; Shih, W.-H.; Pourrezaei, K.; Robinson, M. K.; Adams, G. P. *Anal. Chem.* **2011**, *83*, 3392-3397.
(39) Ngamcherdtrakul, W.; Castro, D. J.; Gu, S.; Morry, J.; Reda, M.; Gray, J. W.; Yantasee, W. *Cancer Treat. Rev.* **2016**, *45*, 19-29.
(40) Chun, L.; Kim, S.-E.; Cho, M.; Choe, W.-s.; Nam, J.; Lee, D. W.; Lee, Y. *Sens. Actuator. B Chem.* **2013**, *186*, 446-450.
(41) Ohno, Y. F., H.; Goto, A.; Nakamura, A.; Nishiura, Y.; Sugiura, T.; Ohira, Y.; Yoshioka, T.; Goto, K. *Int J Med Sci* **2013**, *10*, 1286-1294.
(42) Kapeller, B. M., J.; Losert, U.; Podesser, B. K.; Macfelda, K. *ESC Heart Fail* **2016**, *3*, 122-130.
(43) Poghossian, A.; Weil, M.; Cherstvy, A. G.; Schoning, M. J. *Anal Bioanal Chem* **2013**, *405*, 6425-6436.
(44) Abouzar, M. H.; Poghossian, A.; Cherstvy, A. G.; Pedraza, A. M.; Ingebrandt, S.; Schoning, M. J. *Phys Status Solidi A* **2012**, *209*, 925-934.

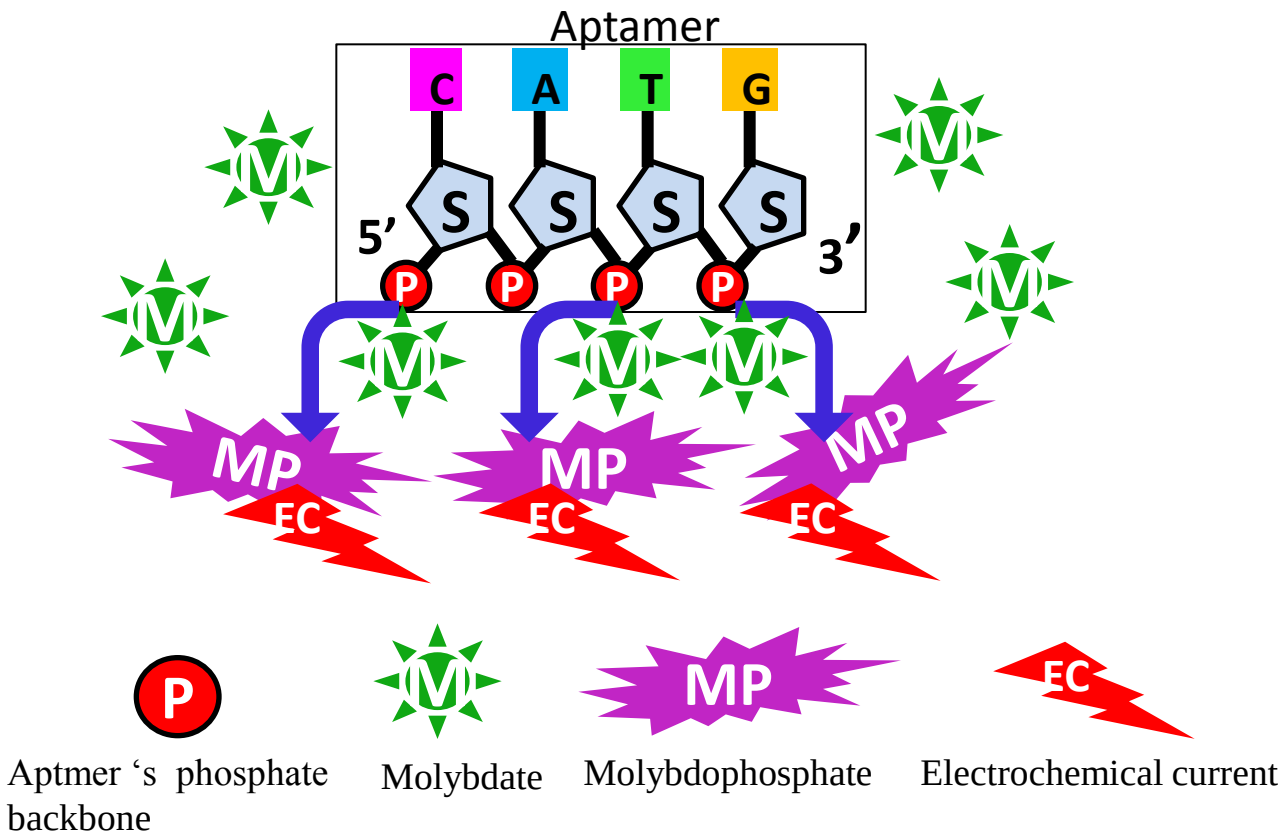
Aptamer
C
A
T
G
S
S
S
S
5'
3'
P
P
P
P
M
M
M
M
M
M
MP
MP
MP
EC
EC
EC
P
M
MP
EC
Aptmer 's phosphate backbone
Molybdate
Molybdophosphate
Electrochemical current

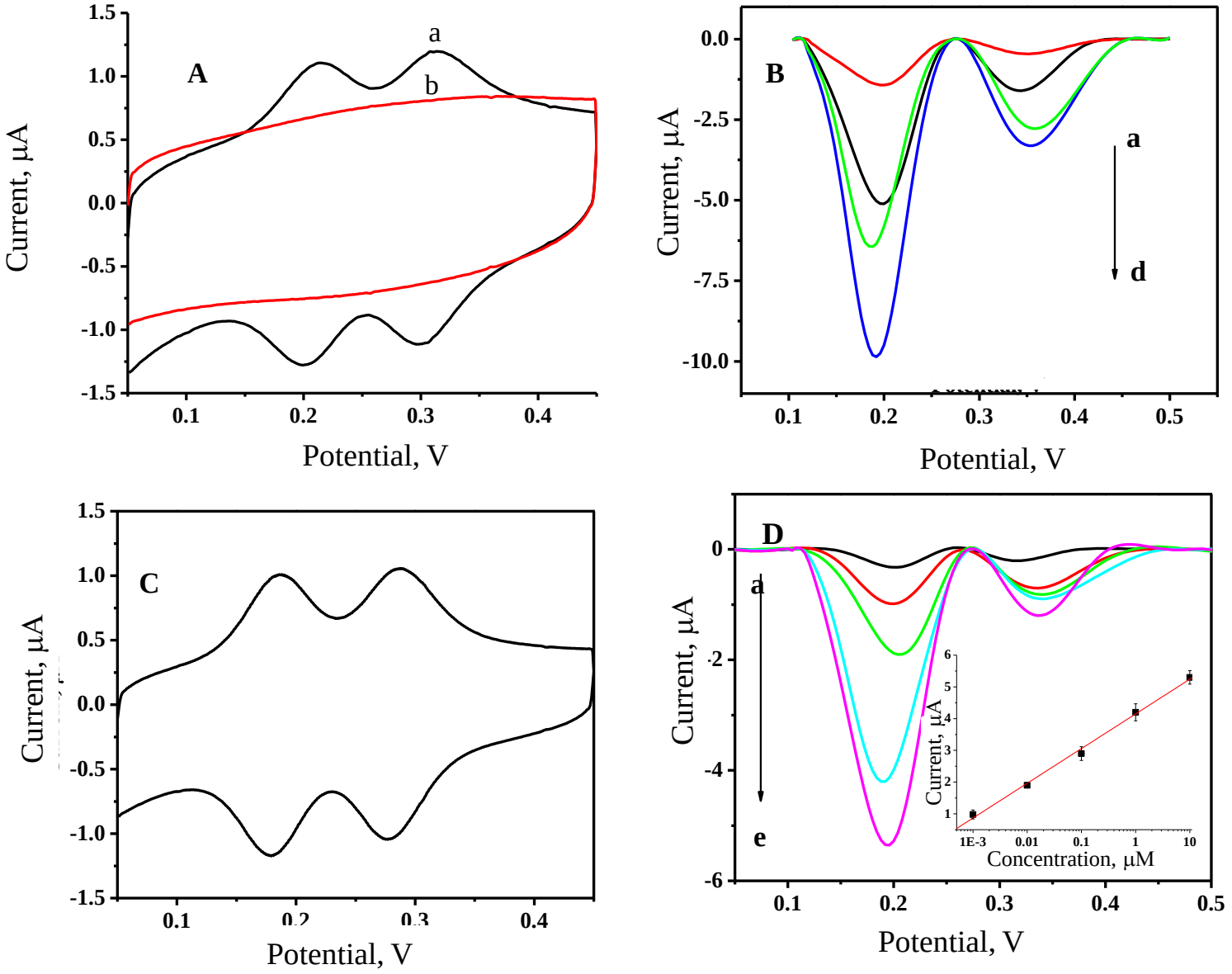
A
a
b
Current, μA
Potential, V
B
a
d
Current, μA
Potential, V
C
Current, μA
Potential, V
D
a
e
Current, μA
Concentration, μM
Current, μA
Potential, V

Figure 1

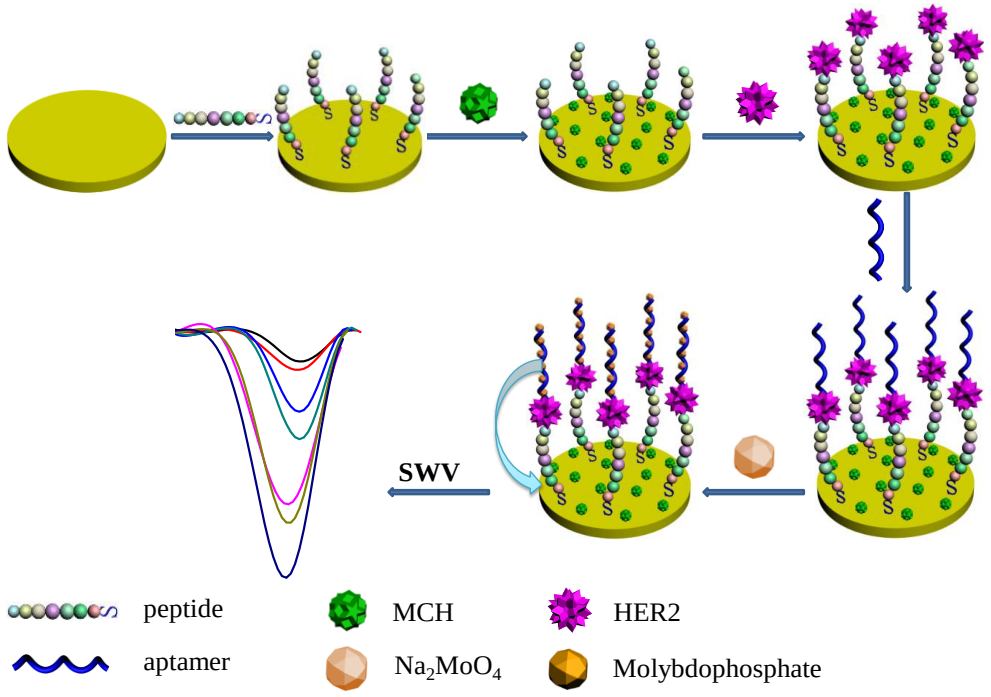

Figure 2

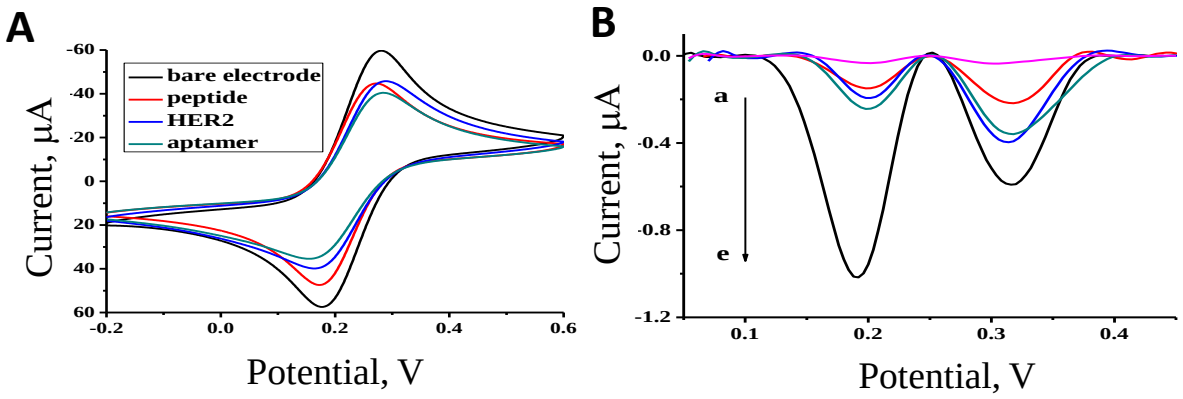
A
bare electrode
peptide
HER2
aptamer
Current, μA
Potential, V
B
a
e
Current, μA
Potential, V

Figure 3

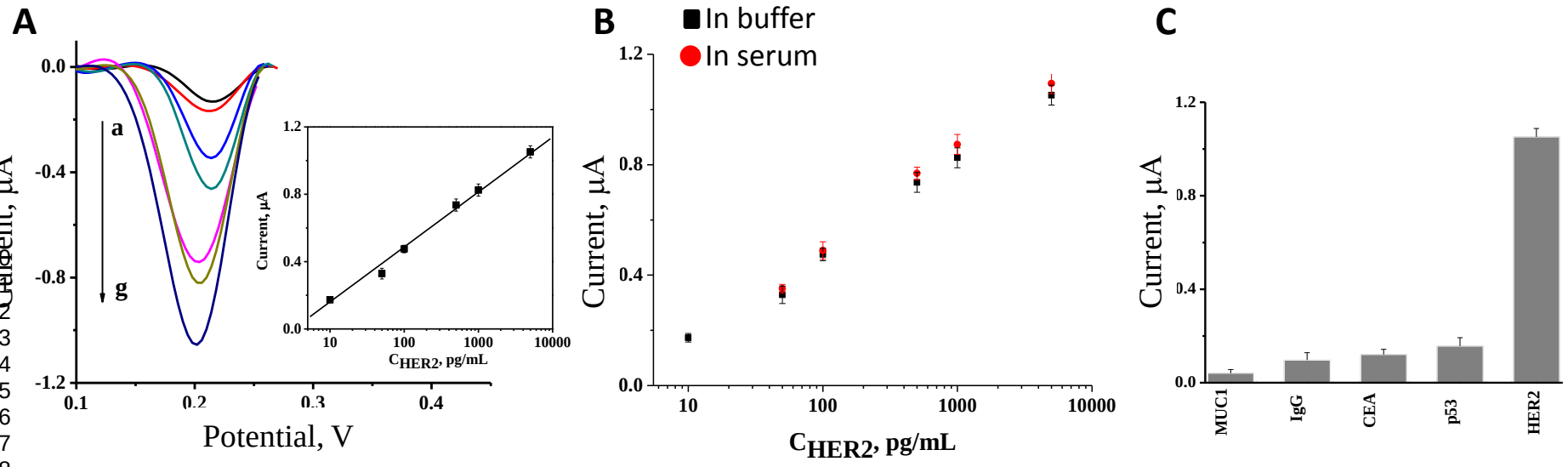
A
Current, μA
Potential, V
a
g
Current, μA
C_{HER2}, pg/mL
B
In buffer
In serum
Current, μA
C_{HER2}, pg/mL
C
Current, μA
MUC1
IgG
CEA
p53
HER2

Figure 4